INSERTING SIMULATED TRACKS INTO SAR CCD IMAGERY

Eric Turner *

University of California, Berkeley
Berkeley, California 94720 USA
elturner@eecs.berkeley.edu

Rhonda D. Phillips, Carol Chiang, Miriam Cha

MIT Lincoln Laboratory
Lexington, Massachusetts 02420 USA
{rhonda.phillips,chiang,miriam.cha}@ll.mit.edu

Keywords: Synthetic aperture radar, line detection, SAR simulation, change detection

Abstract

Synthetic Aperture Radar Coherent Change Detection (SAR CCD) images are highly sensitive change maps produced by multiple SAR images. The noise and characteristics of SAR and CCD result in SAR CCD images being challenging to interpret, making human analyst training essential. Simulating a SAR and CCD dataset with realistic noise is an unsolved problem, and collecting real data with a wide variety of scenarios is challenging and error prone. In this paper, we introduce two algorithms to insert tire tracks and footprints (simulated activities) into existing, non-simulated CCD images. In the first approach, we directly insert synthetic tracks that are modeled to characterize the appearance of tire tracks and footprints into existing CCD images. In the second approach, we use a phase-shift technique prior to CCD formation, providing more realistic activity signatures at an increased computational complexity. The position of the tire tracks and footprints are determined using a simulation software application such as Joint Semi-Automated Forces (JSAF), allowing this SAR CCD simulation capability to be integrated into a larger overall system. In this paper, we provide a full description of the algorithms and the integration into a software system, and we provide experimental results showing the simulated CCD image output with comparisons between the two approaches.

1. INTRODUCTION

Synthetic Aperture Radar Coherent Change Detection (SAR CCD) is a sensitive change detection capability that is challenging to collect and interpret. The interpretation challenge stems from the presence of noise due to the statistical nature of SAR and CCD and the subtlety of features of interest, such as foot tracks. The collection challenges arise from the costs associated with such a data collection, the difficulty in processing the data to form the images, and the uncertainty associated with feature detection in SAR CCD. CCD requires two nearly identical SAR images, which in turn require two nearly identical flight paths. If these paths are close enough, the resulting SAR images can be formed, registered, and aligned in the phase dimension to form CCD images. In order to acquire CCD images with features of interest such as tracks, ground actors are required to make the required tracks. Even if appropriate scripted activities are executed on the ground, there is no guarantee that these features will be present in the resulting CCD images, as the appearance of changes is dependent on the processing, ground characteristics, weather, and sensitivity of the radar. These interpretation and collection challenges are conflicting, as acquiring good data for the purposes of training human analysts and algorithms is difficult.

Although models exist to simulate the appearance of SAR images, there are no existing models for generating CCD images with interesting features. CCD images have complicated noise characteristics, and many environmental factors contribute to the overall appearance. Simulating a realistic CCD background would be highly challenging. Inserting realistic ground features into existing SAR CCD images, however, is manageable, produces realistic SAR CCD images, and enables the creation of test data that contains a wide range of features of interest. The contribution of this paper is to introduce a model-based method for inserting interesting and realistic features into existing CCD images. In order to assess whether the features are realistic, we evaluate them based on similarity to real features. In the following Section, we provide a background on SAR CCD processing.

2. BACKGROUND

One of the challenges in acquiring good SAR CCD data is in the sensitive processing required to form the change images. CCD uses a traditional interferometry technique that utilizes phase information of two (or more) SAR images collected from nearly identical geometries to detect small (sub-

*This work is sponsored by the Department of Defense under Air Force Contract FA8721-05-C-0002. Opinions, interpretations, conclusions and recommendations are those of the author and are not necessarily endorsed by the United States Government.

wavelength) changes in ground surface height between collections [1].

The formation of a CCD image begins with the collection and formation of two or more SAR images from identical collection geometries (using identical flight paths) [1]. Autofocus is a typical processing step in the formation of SAR images that sharpens the images around prominent scatterers in the scene. Care should be taken to jointly autofocus both SAR images so that pixel intensities for the same features will match [2]. The next challenging step is the geometric registration of the images in order to form pixel-level change images. SAR CCD formation assumes that identical collection geometries are used to ensure that the phase in the two images are aligned. If this is the case (the airborne platform flight paths are the same), differences in phase are due to changes on the ground. As collection geometries are not identical in practice due to natural variations in flight paths, aperture trimming in Fourier space is necessary to correct slight phase differences caused by differences in collection angles [2]. This processing can correct small errors in phase, but large differences between collection geometry will decrease overall coherence, making images difficult or impossible to interpret.

The calculation of the estimated coherence is straightforward, but there are issues related to using coherence as a metric for change. The coherence between two complex pixels in two SAR images can be estimated using the complex correlation coefficient in a neighborhood around the pixels [1]. Several factors influence coherence, including misaligned SAR data and natural variations in foliage on the ground. This makes change detection and image interpretation difficult. Furthermore, estimated coherence is a biased random variable with a large variance for small coherence values [3]. Any change on the ground such as a tire track would therefore have a mixture of dark and light pixel values instead of having solid black lines. If the underlying surface is naturally noisy or impenetrable, resulting in vehicle tracks that are not observable, the tracks are unlikely to be observable in a CCD image. Because there are many obstacles to collecting and forming good CCD data with observable features of interest, we will focus on inserting those features once we have good, reliable data.

3. TRACK INSERTION ALGORITHMS

There are two natural approaches for inserting tracks into SAR CCD images: altering the phase information prior to CCD formation and altering the pixel/coherence values in final CCD images. Altering pixel values in CCD images does not require any additional data such as the original SAR images, but does require a good model for track/feature appearance. The other approach requires more data, but does not require a good CCD appearance model. In the following Subsections, we describe both approaches in detail.

3.1. Description of Post-CCD Algorithm

To begin, we assume we are given a raster image $\gamma \in [0,1]^{m \times n}$ that represents the result of calculating the CCD of two SAR images, along with a list of pixel locations. Given pixel locations in the original CCD images, our goal is to insert a realistic synthetic track. The following describes the model used to characterize the appearance of tire tracks and footprints in SAR CCD images. The images used in this paper were collected using a Boeing Compact Ku-band radar.

3.1.1. Tire-track appearance model

Observing Figure 1, tire tracks in CCD imagery have lower coherence than the surrounding terrain, and appear to vary randomly in intensity. This variance can be explained by environmental properties, such as background coherence, geometry of the vehicle, nature of the terrain (hard or soft soil), as well as radar characteristics.

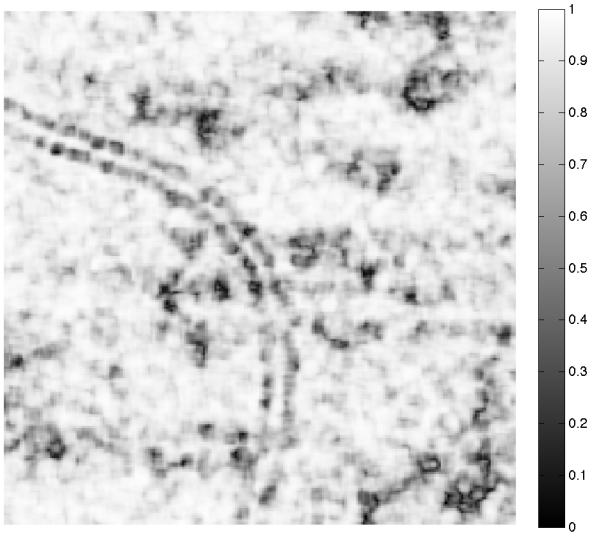

Figure 1. Example tire tracks in a SAR CCD image.

Our goal is to parameterize the appearance of tire tracks, providing a realistic model without unnecessary complexity. Upon inspection, one can characterize the pattern of a tire-track with a sequence of rectangles in-line with the path orientation (see Figure 2). By determining the probability distributions of all parameters that determine the placement and geometry of these rectangles (or "blocks"), one can then create new tracks with the same characteristics.

Given the assumption that there are two parallel tire tracks with separation s (measured in pixels), Figure 3 represents all information necessary to define the position of a track block given the position of the previous block. Table 1 defines the set of parameters along with example distributions for each parameter of CCD images with a pixel resolution of 0.15 me-

Figure 2. Close-up of tiretracks in SAR CCD image (left) with outline of each block (right)

ters/pixel. These parameters were chosen by experimentation for a specific radar geometry set.

Note that the intensity of each block is not represented by a constant-height rectangle, but rather is initially represented as a pyramid with an offset peak. The location of this peak within the pyramid is represented by the parameters *mx* and *my*. Note that this peak will represent a maximum intensity value.

Using the above parameters, the pixel intensities of an individual tire-track can be generated in a blank image (background of zero intensity). Note that the track components must be sheared and rotated to match the specified paths curvilinear profile. Once the resulting image is created, it can be passed through a rudimentary low-pass filter to create more realistic block geometry.

Note that the average coherence along a track is lower than the local average image coherence, even in locations that do not contain a noticeable block. This effect can be modeled by adding additional layers of blocks attenuated by some factor. Thus two separate tracks are generated for each path, where the second track is scaled, and the results are added together. The intensity-scaling factor for the second set of blocks used in the above example is 0.4.

At this stage, a track with positive intensities exists on a background of zero intensity. Note that the track so far is independent of the coherence in the original image. In order to model environmental effects on the tire tracks, this image can be scaled element-wise by the original CCD image, γ. The result is that areas of low coherence in the CCD image are less affected by the track disturbance. Finally, the track image is subtracted from γ, giving the modified CCD image. If we let $T_i \in [0,1]^{m\times n}$ be defined as a single layer of blocks, and h be defined as a low-pass filter, then the modified CCD image, γ', can be defined as:

$$\gamma' = \gamma \;-\; \gamma \times \Big((T_1 + 0.4\,T_2) * h\Big), \tag{1}$$

where $\times$ represents element-wise multiplication, and $*$ represents two-dimensional convolution. Figure 4 shows the result of this process, where each of the Random Variables in Table 1 are modeled with uniform distributions.

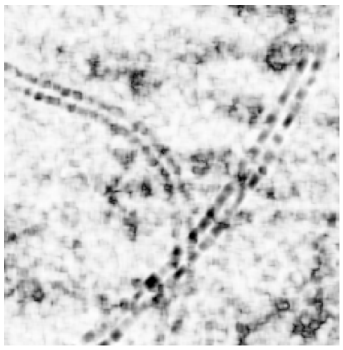

Figure 4. Artificial track (with parameters specified in Table 1) inserted into Figure 1

3.1.2. Footprints appearance model

Footprints can be formed using the same model as above, with modified distributions for each parameter. Also note that the parameters W and s are not necessary in this case. Table 2 is an example set of parameters for footprints. Again, the example values given were chosen experimentally.

Figure 5. Real footprints (top two horizontal lines) with artificial footprints (bottom line)

Note that footprints are much fainter that tire tracks. Figure 5 shows an image with three sets of footprints. The top two are real footprints, while the bottom is a synthetic track that is an example of the above parameter set.

3.2. Description of Pre-CCD Algorithm

Rather than modeling the appearance of CCD as in the previous Subsection, we can randomly alter the SAR phase to induce artificial changes. A CCD image is computed from two existing SAR images, $S_1, S_2 \in \mathbb{C}^{m\times n}$. The earlier image S_1 is often referred to as the "reference" image while S_2, which was taken after some change occurred, is referred to as the "change" image. The coherence of a pair of complex SAR images is defined as:

$$\gamma(x,y) = \frac{E\Big[\,|\,S_1(x,y)S_2(x,y)^*\,|\,\Big]}{\sqrt{E\Big[S_1(x,y)^2\Big]E\Big[S_2(x,y)^2\Big]}} \tag{2}$$

Where $E[...]$ represents statistical expected value. Since the CCD algorithm is performed on a finite-sized image, an estimator for the expected value is used,

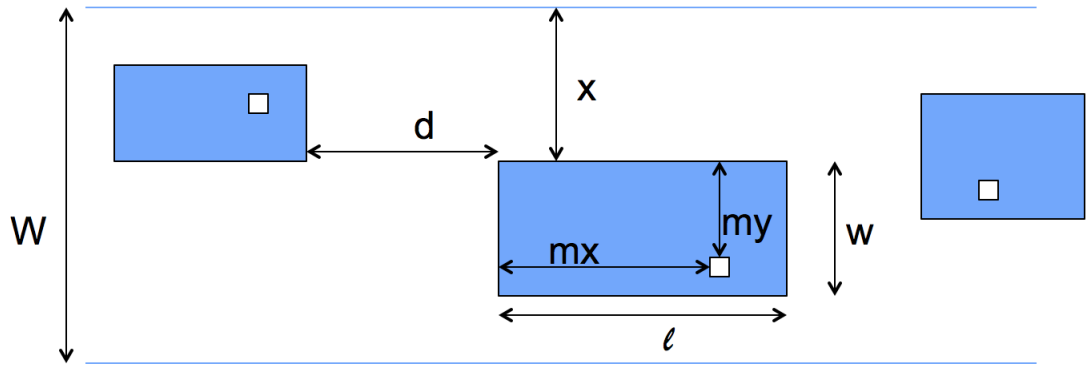

Figure 3. Definition of track parameters

Table 1. Tire-Track Parameters and Example Distributions

Parameter	Description	Mean	Variance
W	Width of track	5 (*pixels*)	n/a
s	Distance between tiretracks	2 (*pixels*)	n/a
d	Along-track distance between blocks	4 (*pixels*)	12 ($pixels^2$)
x	Cross-track offset of block	8 (*pixels*)	5.33 ($pixels^2$)
l	Length of block along track	6 (*pixels*)	1.33 ($pixels^2$)
w	Cross-track width of block	8 (*pixels*)	5.33 ($pixels^2$)
m	Maximum intensity of block (measured from zero intensity)	0.3 (intensity value)	0.0133
mx	The along-track location of the peak of block intensity	0.8 (percentage of l)	0.03
my	The cross-track location of the peak of block intensity	0.5 (percentage of w)	0.00333

Table 2. Footprint Parameters and Example Distributions

Parameter	Description	Mean	Variance
d	Along-track distance between blocks	15 (*pixels*)	40.33 ($pixels^2$)
x	Cross-track offset of block	0 (*pixels*)	1.33 ($pixels^2$)
l	Length of block along track	4.5 (*pixels*)	2.083 ($pixels^2$)
w	Cross-track width of block	4.5 (*pixels*)	2.083 ($pixels^2$)
m	Maximum intensity of block (measured from zero intensity)	0.2	1.267
mx	The along-track location of the peak of block intensity	0.8 (percentage of l)	0.03
my	The cross-track location of the peak of block intensity	0.5 (percentage of w)	0.00333

$$\hat{\gamma}(x,y) = \frac{\Sigma_{k=1}^{N} \mid S_1(x_k,y_k)S_2(x_k,y_k)^* \mid}{\sqrt{\left(\Sigma_{k=1}^{N} S_1(x_k,y_k)^2\right)\left(\Sigma_{k=1}^{N} S_2(x_k,y_k)^2\right)}} \quad (3)$$

Note that the numerator effectively performs an inner product on a sub-region of the two respective regions, while the denominator normalizes by the magnitude of these sub-regions. Since the inner product is proportional to the magnitude of each sub-image, the resulting value is primarily dependent on the relative phase between the two images. Thus if one wanted to artificially reduce the coherence of a particular region, one might naïvely perform a uniform phase-shift of the values in that region in the mission SAR image. This approach is not an effective way to adjust the magnitude of γ. Consider the following example.

3.2.1. Constant Phase-Shift Example

Assume for the simple case where the mission and change images are perfectly aligned: $\forall x,y : S_1(x,y) = S_2(x,y)$. This means the CCD image has a magnitude of 1 at every pixel, indicating perfect coherence. Our goal is to artificially lower the coherence in a particular region by shifting the phase of that region by some angle, $\Delta\theta$.

Define $S_1(x,y) = |S_1(x,y)|e^{i\angle(S_1(x,y))}$ and $S_2(x,y) = |S_2(x,y)|e^{i\angle(S_2(x,y))}$. For a pixel (x,y) contained in this modified region (sufficiently far from the edge of the region), it can be shown:

$$\hat{\gamma}(x,y) = \frac{|\ \Sigma_{k=1}^{N}\ |S_1(x_k,y_k)|e^{i\angle(S_1(x_k,y_k))}\ \ |S_2(x_k,y_k)|e^{i(\Delta\theta-\angle(S_2(x_k,y_k)))}\ |}{\sqrt{\left(\Sigma_{k=1}^{N}S_1(x_k,y_k)^2\right)\left(\Sigma_{k=1}^{N}S_2(x_k,y_k)^2\right)}}. \quad (4)$$

Since $\forall k \in [1,N] : S_1(x_k,y_k) = S_2(x_k,y_k)$:

$$\hat{\gamma}(x_k,y_k) = \frac{|\ \Sigma_{k=1}^{N}\ |S_1(x_k,y_k)|^2 e^{i\Delta\theta}\ |}{\Sigma_{k=1}^{N}S_1(x_k,y_k)^2} = |\ e^{i\Delta\theta}\ | = 1. \quad (5)$$

Thus the result still has a magnitude of 1. Since the phase of the coherence is not typically used, this technique is not an effective way to artificially insert disturbances. This method will reduce the coherence in the image, but only due to edge effects along the region of disturbance.

3.2.2. Algorithm Description

To achieve realistic disturbances in CCD using a phase-shift approach, a random variable is added to the phase of each pixel desired instead of a deterministic phase-shift within the selected region of the SAR mission image. By varying the phase shift pixel-by-pixel, deconstructive interference is introduced in the summation in the numerator of (3), while the value of the denominator remains constant, effectively reducing the coherence. In practice, additive Gaussian white noise was chosen for this algorithm in order to mimic natural disturbances within the SAR image. By adjusting the variance of this noise, the intensity of the artificial track can be adjusted, allowing flexible control of image editing.

Figure 6 compares the results of the above approach with a constant phase shift. Note that the vertical lines on the left-hand side were generated using Gaussian noise of increasing variances and the right-hand side lines were generated using a constant phase shift with increasing shift angles. The center of each horizontal track has high coherence, with low coherence around the edges. When adjusting the phase of the modified region by a constant amount, only edge effects along that region appear in the resultant CCD magnitude.

Selecting an intensity that is appropriate for the image, one can mimic the appearance of tire tracks. In Figure 7, there are two sets of tire tracks. The left-hand set exists in the original image, while the right-hand set is artificially inserted into the image in post-processing using the above technique. These artificial tracks display the same pattern as those created using the post-CCD algorithm described in Section 3.1, even though the phase mask does not contain any information about "blocks."

3.3. Interfacing with Simulation Software

In order to insert physically realistic tracks, we leverage existing models contained in Joint Semi Automated

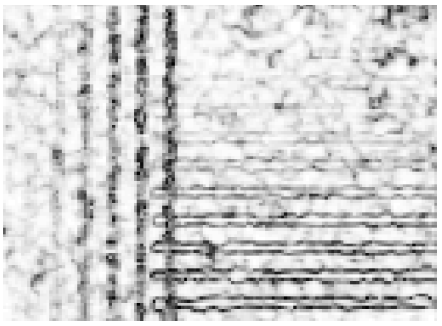

Figure 6. Artificial insertion by Gaussian phase shift (left) and deterministic constant phase shift (right)

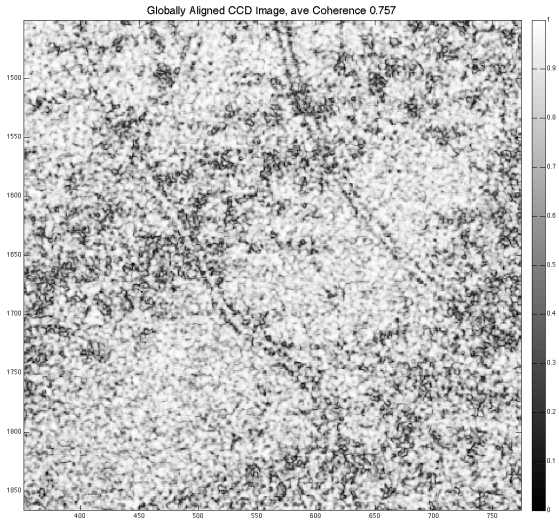

Figure 7. Original tire tracks (left) verses artificial tire tracks (right)

Forces (JSAF) [4]. JSAF is a Computer Generated Forces (CGF) application that descended from Modular Semi Automated Forces (ModSAF) [5]. It has a collection of models—vehicles, dismounted infantry (DI), weapons, as well as human behaviors—and tools for simulating a battlefield environment. Our simulation system leverages a network packet recorder to capture the simulation data in order to input to our SAR CCD simulation. This provides an easy mechanism to transfer data from a networked simulation system and our algorithm. From the recorded file, we extracted the location (latitude, longitude, and altitude), whether the entity was a dismount, and whether it was currently "mounted," i.e., on a vehicle. Knowing whether a dismount is currently on a vehicle is important so that additional foot prints are not drawn.

To create the data shown in Figure 9, we created the JSAF scenario (shown in Figure 8) and recorded the locations of

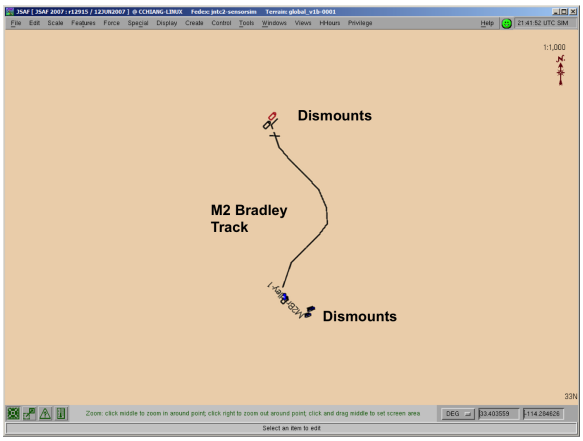

Figure 8. Scenario generated by JSAF simulation.

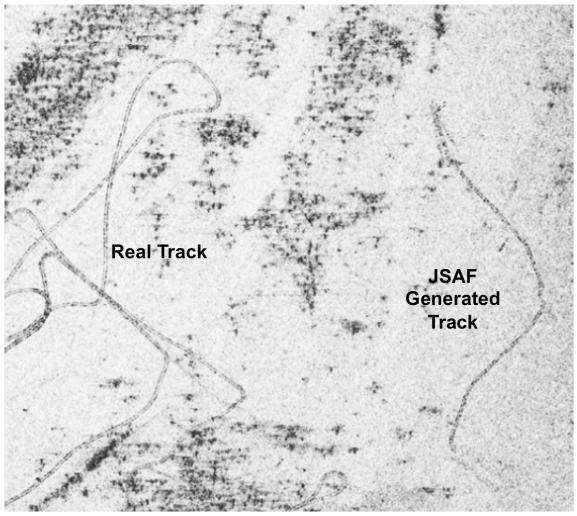

Figure 9. Real CCD image with JSAF scenario inserted.

tire tracks and footprints. The scenario included a Squad of DI walking up to an M2 Bradley Fighting vehicle. They mounted the M2, which then drove a short distance. When the M2 stopped driving, the DI dismounted and walked away from the M2. Using the Post CCD algorithm, tire tracks and footprints were inserted onto the right side of Figure 9. The left side of the figure shows actual tire tracks/footprints. By visually comparing the real and synthetic tracks in the same image, we determine that the synthetic tracks match the real tracks in appearance.

4. ANALYSIS

In this Section, we develop and apply two different analysis approaches to determine how closely the synthetic features match real features. The first approach, a statistical analysis, measures the statistics of synthetic tracks and compares those values to the measured statistics of actual tracks. A second method of analysis leverages an automatic track detector to compare the rate of detection of synthetic tracks to real tracks. This analysis is especially important in determining the suitability of synthetic feature data for algorithm development. The following describes the results of these two approaches on the synthetic injection techniques.

4.1. Statistical Approach

By comparing the relevent statistics of authentic and synthetic tracks, one can determine whether both types of tracks have the same characteristics. Tracks must be separated from the rest of the image before extracting statistical information, so that background clutter is not considered part of the track. This separation is performed spatially by tracing across the track and keeping all pixels that fall within a certain distance from the track center. For synthetic tracks, this tracing is accomplished using the defining path of the track. For actual tracks, the tracing is placed either by hand or by a line-finding algorithm.

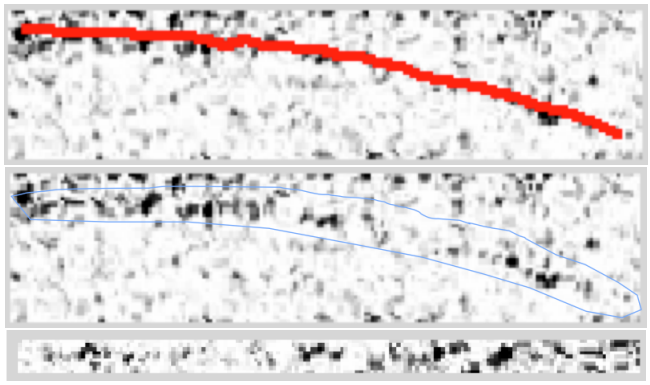

Figure 10. Straightening a track from a trace.

Figure 10 shows the case where the image within 4 pixels to either side is kept as part of the track. This track is detected using a line-finding algorithm, and the width of four pixels allows for the full track to be represented (a single tire from a vehicle), while limiting the amount of background clutter in the trace.

The following analysis considers the sample mean and standard deviation for each track obtained. These parameters are sufficient to show a separation between tracks and non-track regions as well as show the similarities between real and synthetic tracks.

As a test set, 1642 potential tracks were obtained from a SAR CCD dataset. These potential tracks include authentic tire tracks and footprints, synthetic tire tracks and footprints, as well as false positives including random regions of high and low coherence, as well as linear artifacts that occurred during SAR processing.

Figure 11 plots the mean and standard deviation of the intensity of these data graphically. Note that since all values

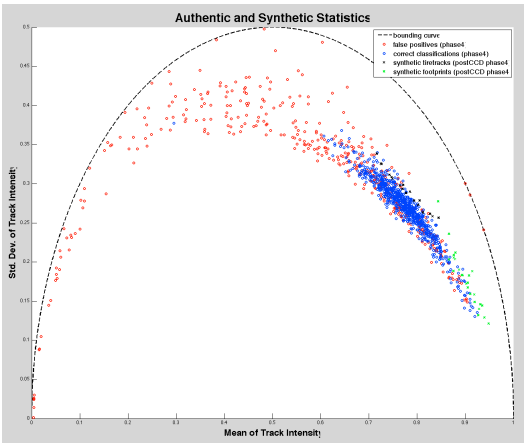

Figure 11. Plotting mean and standard deviation of acquired tracks and non-track regions

within the CCD image are within the range $[0,1]$, there exists a maximum standard deviation associated with each mean. For a given mean μ, a track whose pixels are composed of samples of a Bernoulli distribution with success probability $p = \mu$ will yield this maximum standard deviation, which is shown in Figure 11 with a dotted line.

Each point on this figure represents the statistics for a potential track. Note that the tracks only occupy a small portion of this region. This clustering indicates properties of the CCD image, such as contrast and average coherence. The red points represent false classifications of linear artifacts in the imagery that were not tracks, while the blue points represent actual tire tracks.

This plot shows that falsely classified linear features have a lower mean intensity than actual tracks. The black and green points represent synthetic tire tracks and footprints, respectively, which have been inserted into the CCD imagery. The cluster of synthetic tire tracks overlaps with actual tire tracks found, and the cluster of synthetic footprints lies with higher mean intensity on the same curve. This is to be expected, since footprints have a lighter average intensity. Thus this pair of statistics indicates that the described synthetic tracks have similar statistical properties to authentic tracks.

4.2. Track-Finding Algorithm Analysis

Since an application of synthetic track insertion is to create realistic training data for algorithms whose input is SAR CCD imagery, one potential metric of quality for synthetic tracks is their rate of detection by existing line-finding algorithms. If the rate at which a sample track is detected is equivalent to the rate of detection of authentic tracks, then synthetic and authentic tracks are indistinguishable in the context of these algorithms.

The line detection algorithm used in this analysis was developed by MIT Lincoln Laboratory, and the algorithm segments each image into 250×250 pixel (corresponding to 25×25 m) subregions. In each region, a hypothesis test is conducted to determine whether a line exists at angle θ and offset d, testing 10,000 possible pairs of these values.

Several test images that contain existing tracks were used for this analysis. Artificial tracks were inserted into these images. The shape and intensity of the inserted tracks is matched to the existing tracks. Since the line detection algorithm used assumes straight linear features, the curvature of a track greatly affects its detectability. Figure 12 highlights a situation where the synthetic track has a curvature of zero, which is much easier to detect than the authentic track even though it is laid on top of a region of lower coherence. Figure 13 shows an example where a synthetic track has been inserted in order to mimic the curvature characteristics of an authentic track.

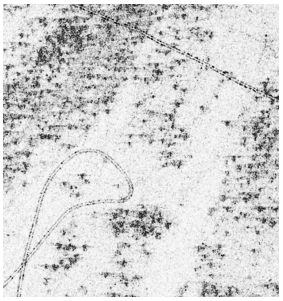

Figure 12. Example input to line-finding analysis. Authentic track is in lower left, while synthetic track is inserted across upper-right. Note that the synthetic track has a lower curvature value, which makes it more detectable to a linear feature-finding algorithm.

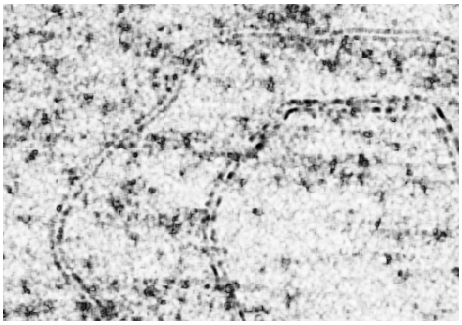

Figure 13. In this input to the line-finding analysis, the synthetic track (featured below the original track) was formed to mimic the curvature and intensity of the original track.

The test set of images used has synthetic tracks that match the curvature of existing tracks. In order to provide a score for this analysis, the line detection algorithm is run on the test images, and each line that corresponds to a track (authentic or synthetic) is retained. For each authentic track in the test

set, there exists a synthetic track that mimics it, creating N pairs of these tracks in total. Thus, for synthetic-authentic pair $k \in [1,N]$, let $s_k = 1$ if the synthetic track was tagged, and $s_k = 0$ if it was missed. Similarly, let $a_k = 1$ if the authentic track was tagged, and $a_k = 0$ if it was missed. Thus a scoring metric is:

$$score = \frac{1}{N} \sum_{k=1}^{N} (s_k - a_k). \quad (6)$$

A score close to zero is desired. Scores close to ± 1 indicate that the track finder is biased towards either synthetic or authentic tracks. Note that this scoring metric will return zero if, for one pair, only the synthetic track is found, and for another, only the authentic track is found. This is intentional, since it corrects for the effects of local background disturbances that could cause only one track to be detected, even though they have the same curvature or average background intensity.

For the 73 track pairs tested, the resulting score was -0.0411. The overall track recall rate was 19.8%, where 24.7% of the all tracks considered were in areas of low coherence, and the total percentage of track pairs that satisfied $a_k = s_k$ was 71.2%. This analysis indicates that the synthetic tracks closely resemble authentic tracks.

5. CONCLUSION

This paper demonstrates two techniques used to insert synthetically generated tracks into existing SAR CCD images. Both of these techniques are verified using statistical comparisons between synthetic tracks and existing tracks. Additionally, linear detection algorithms were used to compare the detectability of each type of track. This analysis resulted in confirmation that synthetic and authentic tracks are equally detectable.

Several areas discussed in this paper can be the focus of future work. The pre-CCD track insertion algorithm introduced in Section 3.2 generates features by adding stationary Gaussian noise to existing phase values in the mission SAR image. This initial approach yielded realistic results, but a more complex insertion technique may yield an even more accurate product. Additionally, further statistics could be considered in the analysis of these insertion techniques, in addition to the mean and variance of the intensity of tracks. Considering relational statistics, such as the auto-correlation function of a track's intensity, may affirm measured parameters such as block spacing in the insertion algorithms.

Finally, note that a goal for the development of these algorithms is to generate publically available SAR CCD datasets. There exist SAR CCD data in the public domain, yet these sets contain very limited instances of footprints or tire tracks and do not include groundtruth position data [6]. In conjunction with the algorithms described in this paper, the existing images in these sets can be used to create suitable data for algorithm development and analyst training.

6. ACKNOWLEDGEMENTS

This work was sponsored by the ASD (Research and Engineering)'s Rapid Reaction Technology Office.

REFERENCES

[1] C.V. Jakowatz, Jr, D.E. Wahl, P.H. Eichel, D.C. Ghiglia, and P.A. Thompson. *Spotlight-mode Synthetic Aperture Radar: A Signal Processing Approach*, chapter 5. Kluwer Academic Publishers, Norwell, MA, 1996.

[2] A.W. Doerry. SAR data collection and processing requirements for high quality coherent change detection - art. no. 694706. *Radio Sensor Technology XII*, 6947:94706–94706, 2008.

[3] R. Touzi, A. Lopes, J. Bruniquel, and P.W. Vachon. Coherence estimation for SAR imagery. *IEEE Trans. Geosci. Remote Sens.*, 37(1):135–149, 1999.

[4] A. Ceranowicz, P. Nelson, and F. Koss. Behavioral representation in JSAF. In *Proceedings of the Ninth Conference on Computer Generated Forces*, University of Central Florida, 2000. Paper 9TH-CGF-058.

[5] A. Ceranowicz. Modular semi-automated forces. In *1994 Winter Simulation Conference Proceedings*, pages 755–761, December 1994.

[6] S.M. Scarborough, L. Gorham, M.J. Minardi, U.K. Majumder, M.G. Judge, and L. Moore. A challenge problem for SAR change detection and data compression. *SPIE*, 2010.